Downlink Performance Analysis for a Generalized Shotgun Cellular System

Prasanna Madhusudhanan, Juan G. Restrepo, Youjian Liu, *Member, IEEE*,
Timothy X Brown, and Kenneth R. Baker, *Senior Member, IEEE*

***Abstract*—In this paper, we analyze the signal-to-interference-plus-noise ratio (SINR) performance at a mobile station (MS) in a random cellular network. The cellular network is formed by base stations (BSs) placed in a one-, two-, or three-dimensional space according to a possibly non-homogeneous Poisson point process, which is a generalization of the so-called shotgun cellular system. We develop a sequence of equivalence relations for the SCSs and use them to derive semi-analytical expressions for the coverage probability at the MS when the transmissions from each BS may be affected by random fading with arbitrary distributions as well as attenuation following arbitrary path-loss models. For homogeneous Poisson point processes in the interference-limited case with power-law path-loss model, we show that the SINR distribution is the same for all fading distributions and is not a function of the base station density. In addition, the influence of random transmission power, power control, and multiple channel reuse groups on the downlink performance is also discussed. The techniques developed for the analysis of SINR have applications beyond cellular networks and can be used in similar studies for cognitive radio networks, femtocell networks, and other heterogeneous and multi-tier networks.**

***Index Terms*—Cellular systems, cochannel interference, random cellular deployments, fading channels, stochastic ordering.**

I. Introduction

The modern cellular communication network is a complex overlay of heterogeneous networks such as macrocells, microcells, picocells, and femtocells. The base station (BS) deployment for these network can be planned, unplanned, or uncoordinated. Even when planned, the base station placement in a region typically deviates from the ideal regular hexagonal grid due to site-acquisition difficulties, variable traffic load, and terrain. The coexistence of heterogeneous networks has further added to these deviations. As a result, the BS distribution appears increasingly irregular as the BS density grows and is outside standard performance analysis.

Two approaches of modeling have been widely adopted in the literature. At one end, the BSs are located at the centers of regular hexagonal cells to form an ideal hexagonal cellular system. At the other end, the BS deployments are modeled according to a Poisson point process which we refer to as shotgun cellular system (SCS). An in-depth study of Poisson point processes and other stochastic geometric models can be found in [1]–[4]. In [5], we make a connection between the regular hexagonal model and the Poisson process based model on a homogeneous two dimensional (2-D) plane. It is shown that the signal-to-interference ratio, (SIR), of the SCS lower bounds that of the ideal hexagonal cellular system and, moreover, the two models converge in the strong fading regime. The BS deployment in the practical cellular system lies somewhere in between these two extremes, and as noted in [5]–[7], significant insights about the cellular performance can be gained by thoroughly understanding the hexagonal cellular system and the SCSs, especially in the strong fading regime. The hexagonal cellular systems are difficult to study analytically and hence, vast literature on the performance studies of such systems is purely simulation-based. On the other hand, in this paper we demonstrate that the SCSs are extremely amenable to mathematical analysis even for a very general system model. An in-depth analysis of the downlink performance of the SCS is conducted by considering three levels of generality. Firstly, the BS arrangement in the SCS is according to a non-homogeneous Poisson point process in an arbitrary dimension ($l = 1, 2, 3$), which can mimic the BS arrangement in a real cellular system by the appropriate choice of the intensity function of the point process. Secondly, a general model is considered for the path-loss suffered by the BS transmissions, which covers the most-popular power-law path-loss model as well as other models that more accurately capture indoor propagation losses. Thirdly, the fading undergone by the transmitted signals of each BS is modeled as a random variable with any arbitrary distribution that is independent and identically distributed (i.i.d.) across all the BSs, that covers the most commonly used log-normal and exponential distributions, and more.

Prior Work and Our Contributions: A Poisson point process has been adopted in the literature for the locations of nodes in

Manuscript received November 7, 2013; revised March 14, 2014 and July 22, 2014; accepted September 22, 2014. Date of publication October 22, 2014; date of current version December 8, 2014. This work was supported in part by NSF under Grants ECCS-1408604 and IIP 1414250. This paper was presented in part at the IEEE Globecom Wireless Communications Symposium, Honolulu, HI, USA, November 2009. The associate editor coordinating the review of this paper and approving it for publication was A. Kwasinski.

P. Madhusudhanan was with the Department of Electrical, Computer, and Energy Engineering (ECEE), University of Colorado, Boulder, CO 80309-0425 USA, and also with Qualcomm Inc., Boulder, CO 80301 USA (e-mail: mprasanna@colorado.edu).

J. G. Restrepo is with the Department of Applied Mathematics, University of Colorado, Boulder CO 80305 USA (e-mail: juanga@colorado.edu).

Y. Liu is with the Department of Electrical, Computer, and Energy Engineering (ECEE), University of Colorado, Boulder, CO 80309-0425 USA (e-mail: eugeneliu@ieee.org).

T. X Brown is with the Interdisciplinary Telecommunications Program, University of Colorado, Boulder, CO 80309-0422 USA, and also with the Department of Electrical, Computer, and Energy Engineering (ECEE), University of Colorado, Boulder, CO 80309-0425 USA (e-mail: timxb@colorado.edu).

K. R. Baker is with the Interdisciplinary Telecommunications Program, University of Colorado, Boulder, CO 80309-0422 USA (e-mail: kenneth.baker@colorado.edu).

Color versions of one or more of the figures in this paper are available online at http://ieeexplore.ieee.org.

Digital Object Identifier 10.1109/TWC.2014.2362516

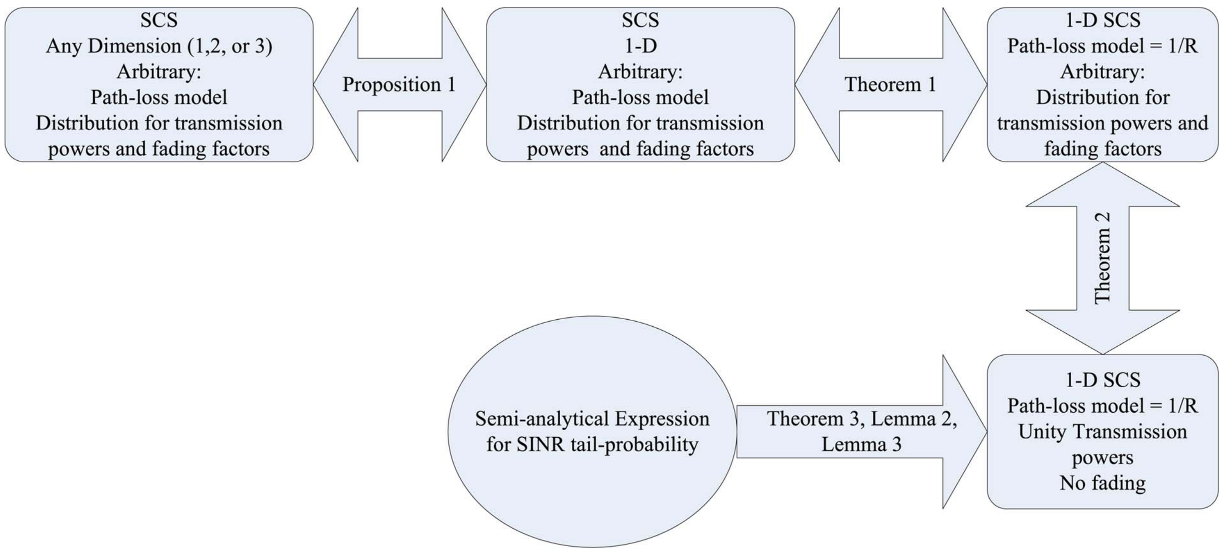

Fig. 1. Contributions of this paper: SINR characterization for SCSs. A general SCS is reduced to the simplest SCS (canonical SCS, lower right corner of the figure) using a series of transformations. The double arrows indicate equivalence of the SINR tail-probability of the SCS before and after the transformation (proved in the theorem that label the corresponding arrows). The SINR tail-probability is derived for the canonical SCS, which is the same for the original SCS as a result of the equivalent transformations.

the study of sensor networks, wireless LANs, cognitive radios, ad hoc networks and other uncoordinated and decentralized networks [8]–[22]. In the case of ad-hoc networks, bounds on the transmission capacity have been derived in several different contexts [23]. Similar outage probability analysis in ad-hoc packet radio networks is considered in [24], [25].

An underlying assumption in all the previous work is that the density of transmitters is constant throughout the cellular region, i.e., the Poisson point process is homogeneous; propagation model follows the power law path-loss; and the fading models are log-normal, Rayleigh, or Rician distributions. In this paper, the three levels of generality mentioned in the previous subsection helps in more accurately modeling the cellular system thereby making the results hold for a wide variety of practical scenarios. Moreover, the region of interest need not be restricted to $\mathbb{R}^2$ as in prior work, and may be $\mathbb{R}^1$ or $\mathbb{R}^3$. Furthermore, the dependence of the downlink performance on the MS location within the cellular region is also characterized. Handoff features and correlations between the fading coefficients corresponding to different BS transmissions are out of the scope of this work.

The main results of this paper are discussed below. As shown in Fig. 1, we successively reduce the actual SCS to a canonical model that is equivalent in terms of the SINR characteristics, and characterize the SINR distribution for the simplest equivalent system, thereby solving the problem for the most general network. These results are covered in Section III borrowing ideas from [17] for constructing the equivalent canonical model. In [17], we looked at a qualitative comparison between the SINRs of two SCSs based on usual stochastic ordering without actually computing the distribution of SINR, whereas in this paper, the main objective is to compute the SINR distribution for any given SCS and to systematically characterize the influence of the model parameters on the downlink performance.

Next, for the special case of homogeneous SCSs, which is the most widely used model for random node locations, the canonical model takes an extremely simple form in which the BS arrangement is according to a unit mean homogeneous Poisson point process and where each BS has unity transmission power and there is no fading. Further, the effect of the system parameters of the actual SCS (e.g., BS density, arbitrary transmission power and fading distributions, background noise power) on the downlink SINR are all captured in the background noise power term in the canonical model. Finally, simple closed form characterizations for the distribution of SINR, downlink coverage (outage) probability, downlink average ergodic rate and several insights about the cellular system are obtainable and are the topic of concern in Section IV.

Applications of the above results to specific wireless communication scenarios are briefly described in Section VI, where we point out the application of the ideas and results of this paper to the performance analysis of cognitive radio networks and heterogeneous and small-cell networks. Next, the system model and the performance metric of interest are briefly explained.

II. System Model

This section describes the various elements used to model the shotgun cellular system, namely, the BS layout, the radio environment, and the performance metrics of interest.

A. BS Layout

Definition 1: The *Shotgun Cellular System (SCS)* is a model for the cellular system in which the BSs are placed in a given l-dimensional plane (typically $l = 1, 2,$ and 3) according to a Poisson point process on $\mathbb{R}^l$ [1], [26].

The intensity function of the Poisson point process is called the BS density function in the context of the SCS. A 1-D SCS models, for example, the BS deployments along a highway. A 2-D SCS models planar BS deployments, and the 3-D SCS models BS deployments in a dense urban area, or wireless

LANs in an apartment building (note that to model urban areas the BS density function might need to be heterogeneous). The 1-D, 2-D, and 3-D SCSs are described using the BS density functions $d(x)$, $d(r,\theta)$, and $d(r,\theta,\phi)$, where $-\infty \leq x \leq \infty$ represents a point in 1-D, and r, θ, ϕ are used to represent a point in polar coordinates, in 2-D and 3-D.

A l-D SCS is said to be homogeneous if the BS density function is a constant over the entire l-D space. A homogeneous 2-D SCS is a common model for the random node placement in many scenarios.

We consider the most general possible description for the wireless radio environment. Let the received power at a distance $r(\geq 0)$ from a given BS be given by

$$P(r) = K\Psi/h(r), \tag{1}$$

where K represents the transmission power and the antenna gain of the BS, Ψ captures the channel fading, and the function $h(\cdot)$ represents a path-loss[1] that a signal experiences as it propagates in the wireless environment. The most commonly used path-loss model is the power-law path-loss model, $1/h(r) = r^{\varepsilon}$, where ε is called the path-loss exponent.

B. Performance Metric

In this paper, we focus on the downlink performance of the SCS. In other words, we are concerned with the signal quality at a mobile-station (MS) within the SCS. The MS is assumed to be located at the origin of the l-D SCS unless specified otherwise. The signal quality at the MS is defined as the ratio of the received power from the serving BS to the sum of the interference powers (P_I), and the background noise power (η), and is called the signal-to-interference-plus-noise ratio (SINR). In an *interference-limited system*, $P_I \gg \eta$ and the signal quality is the signal-to-interference ratio (SIR).

Using (1), the SINR at the MS from a BS at a distance, say R_i, is

$$\mathrm{SINR} = \frac{K_i\Psi_i/h(R_i)}{\sum\limits_{\substack{j=1\\ j\neq i}}^{\infty} K_j\Psi_j/h(R_j) + \eta}, \tag{2}$$

where $\{K_j, \Psi_j\}_{j=1}^{\infty}$ are independent and identically distributed (i.i.d) pairs of random variables representing the transmission power and the channel gain coefficients, respectively, of the j^{th} BS, and $\{R_j\}_{j=1}^{\infty}$ are random variables that come from the underlying Poisson point process that governs the BS placement. Also, the MS associates itself with the BS that has the strongest received signal power (referred to as the serving BS), and can successfully communicate with this BS only if the corresponding SINR exceeds a certain operating threshold, denoted by γ. In this paper, we find the tail probability [i.e., the complementary cumulative density function (c.c.d.f.)] of the SINR, which helps characterize an important performance metric for wireless networks, namely, the coverage probability, i.e., the probability that a MS is able to successfully communicate with the desired BS. The following section presents some necessary results that help simplify and solve the problem.

[1] Following popular convention, we shall refer to the "path-loss model 1/h(r)" throughout this paper, though from the above definition, 1/h(r) is really the "path-gain."

III. SINR Characteristics

As illustrated in Fig. 1, this section presents several equivalence relations on BS density, path-loss model, transmission power and fading that leads to an equivalent canonical SCS model. Then the equivalence relations are used to simplify the analysis of the SINR. The equivalence is defined below.

A. Equivalence of SCSs

Definition 2: Two SCSs are *equivalent* if the joint distribution of the powers from all the BSs of a SCS received at the MS located at the origin is the same as the joint distribution of the other SCS.

As a result, if the noise powers are equal, the SINRs at the MSs in two equivalent SCSs have the same distribution.

The following proposition gives an equivalent 1-D SCS for any l-D SCS. It is a simple consequence of the fact that the path-loss models considered in this paper is a function of only the distance between the MS and a BS, not of the orientation.

Proposition 1: An l-D SCS, $l = 1$, 2, and 3 is equivalent to a 1-D SCS with a one-sided BS density function $\lambda(r)$, $r \geq 0$, calculated below, if other parameters are the same.

- For a 1-D SCS with density function $d(x)$, $-\infty \leq x \leq \infty$, $\lambda(r) = d(r) + d(-r)$.
- For a 2-D SCS with density function $d(r,\theta)$, $\lambda(r) = \int_{\theta=0}^{2\pi} d(r,\theta) r d\theta$.
- For a 3-D SCS with density function $d(r,\theta,\phi)$, $\lambda(r) = \int_{\theta=0}^{\pi}\int_{\phi=0}^{2\pi} d(r,\theta,\phi) r^2 \sin(\theta) d\theta d\phi$.

Next, we show the equivalence between SCS's with path-loss model $\frac{1}{h(R)}$ and SCS's with path-loss model $\frac{1}{R}$, using the concepts of stochastic ordering [26]–[28].

Theorem 1: Suppose $h(r)$, $r \geq 0$ is a monotonically increasing function with derivative $h'(r) > 0\ \forall\ r > 0$ and an inverse $h^{-1}(r)$, $r > 0$. Let R denote the distance between an arbitrary BS and the MS. If all other parameters are the same, then a 1-D SCS with BS density function $\lambda(r)$, $r \geq 0$ and path-loss model $\frac{1}{h(R)}$ is equivalent to a 1-D SCS with BS density function $\bar{\lambda}(r) = \lambda(h^{-1}(r)) \times \frac{d}{dr}h^{-1}(r)$, and path-loss model $\frac{1}{R}$. As a result, if the noise powers are the same, the SINRs at the MSs located at the origin in the two SCSs have the same distribution, i.e., the SINR of (2) satisfies

$$\mathrm{SINR}|_{\lambda(r)} =_{\mathrm{st}} \left.\frac{K_i\Psi_i/\tilde{R}_i}{\sum\limits_{\substack{j=1\\ j\neq i}}^{\infty} K_j\Psi_j/\tilde{R}_j + \eta}\right|_{\bar{\lambda}(r)}, \tag{3}$$

where $\{\tilde{R}_j\}_{j=1}^{\infty}$ is the set of distances of BSs from the MS in the 1-D SCS with BS density function $\bar{\lambda}(r)$ and $=_{\mathrm{st}}$ represents the equivalence in distribution.

Proof: See Appendix A. ■

In other words, from the point of view of SINR distribution, we may restrict ourselves to SCSs with the path-loss model

$\frac{1}{h(R)}$ replaced by the simple path-loss model $\frac{1}{R}$. Next, we show that we may also work only with SCSs where the random transmission powers and fades are replaced with deterministic transmission powers and fading coefficients. In the following theorem, we show the equivalence between SCS's with random transmission power and fading and SCS's with deterministic transmission power and fading.

Theorem 2: A 1-D SCS with BS density function $\lambda(r)$, path-loss model $\frac{1}{R}$, random transmission power K and random fading Ψ that are i.i.d. across all BSs, is equivalent to another 1-D SCS with a BS density function $\bar{\lambda}(r)$, $\frac{1}{R}$ path-loss model, unity transmission power and unity fading. The above is true for arbitrary joint distributions of (K, Ψ) as long as $\bar{\lambda}(r) = \mathbb{E}_{K,\Psi}[K\Psi\lambda(K\Psi r)] < \infty$ holds for all $r \geq 0$, where $\mathbb{E}_{K,\Psi}[\cdot]$ is the expectation operator w.r.t. (K, Ψ). The distributions of the SINRs at the MSs located at the origin of the two SCS's are the same if the noise powers of the MSs are equal.

Proof: See Appendix B. ■

Combining Proposition 1, Theorem 1 and Theorem 2, without loss of generality, we can now restrict our attention to the SINR characterization of the canonical SCS defined below. In other words, the distribution of SINR in a network with arbitrary path-loss model, arbitrary i.i.d. fading, and arbitrary i.i.d. transmission powers on the links can be computed from that of the equivalent canonical SCS.

B. The Canonical SCS

Definition 3: A canonical SCS is a 1-D SCS with a BS density function $\lambda(r)$, $r \geq 0$, unity transmission power and unity fading factors for all BSs in the SCS, and a path-loss model of $\frac{1}{R}$.

For a canonical SCS, the BS closest to the origin is the serving BS and the rest of the BSs contribute to the interference power. The following is an interesting fact.

Lemma 1: The distributions of SINRs at the MS in canonical SCSs with BS density function and noise power of the form $\frac{1}{a}\lambda\left(\frac{r}{a}\right)$, $\frac{\eta}{a}$, respectively, are the same for all $\eta \geq 0$ and $a > 0$. Further, when $\eta = 0$, $\mathrm{SIR}|_{\lambda(r)} =_{\mathrm{st}} \mathrm{SIR}|_{\frac{1}{a}\lambda(\frac{r}{a})}$.

Proof: See Appendix C. ■

As a result, the appropriate scaling of the BS density function will not change the p.d.f. of SINR. Next, we derive expressions for the tail probability of the SINR.

C. SINR Distribution of the Canonical SCS

Theorem 3: The tail probability of SINR at the MS in a canonical SCS, $\mathbb{P}(\{\mathrm{SINR}_{\mathrm{canonical}} > \gamma\})$ is given by

$$\mathbb{P}\left(\{\mathrm{SINR}_{\mathrm{canonical}} > \gamma\}\right) = \begin{cases} \int_{\omega=-\infty}^{\infty} \Phi_{\frac{1}{\mathrm{SINR}_{\mathrm{canonical}}}}(\omega)\left(\frac{1-\exp\left(-\frac{i\omega}{\gamma}\right)}{i\omega}\right)\frac{d\omega}{2\pi}, & \gamma > 0 \\ 1, & \gamma = 0, \end{cases} \tag{4}$$

where $\Phi_{\frac{1}{\mathrm{SINR}_{\mathrm{canonical}}}}(\omega)$ is the characteristic function of $\frac{1}{\mathrm{SINR}_{\mathrm{canonical}}}$ given by

$$\begin{aligned} &\Phi_{\frac{1}{\mathrm{SINR}_{\mathrm{canonical}}}}(\omega) \\ &= \mathbb{E}_{R_1}\left[\exp(i\omega\eta R_1) \times \Phi_{P_I|R_1}(\omega R_1|R_1)\right] \qquad (5) \\ &= \mathbb{E}_{R_1}\left[\exp\left(i\omega\eta R_1\right) \times \right. \\ &\left. \exp\left(R_1 \times \int_{u=1}^{\infty}\left(\exp\left(\frac{i\omega}{u}\right)-1\right)\lambda(uR_1)du\right)\right], \qquad (6) \end{aligned}$$

where $\mathbb{E}_{R_1}[\cdot]$ is the expectation w.r.t. the random variable R_1, which is the distance of the BS closest to the origin, and with the probability density function (p.d.f.) $f_{R_1}(r) = \lambda(r) \times \mathrm{e}^{-\int_{s=0}^{r}\lambda(s)ds}$, $r \geq 0$.

Proof: See Appendix D. ■

2) Special Case: SINR Tail Probability for 0 dB and Higher: Now, we take a minor detour from studying the canonical SCS and consider a 1-D SCS affected by i.i.d. random fading factor with unity mean exponential distribution. For this case, the following theorem gives a simpler expression for the tail probability of SINR when $\gamma \geq 1$.

Lemma 2: For a 1-D SCS with a BS density function $\bar{\lambda}(r)$, $\frac{1}{R}$ path-loss model, unity transmission power, i.i.d. unity mean exponential random variable for fading at each BS, the tail probability of SINR for $\gamma \geq 1$ is given by

$$\mathbb{P}\left(\{\mathrm{SINR} > \gamma\}\right) = \int_{r=0}^{\infty}\bar{\lambda}(r)\exp\left(-\eta\gamma r - \int_{s=0}^{\infty}\frac{\bar{\lambda}\left(s\right)ds}{1+(\gamma r)^{-1}s}\right)dr. \tag{7}$$

Proof: See Appendix E. ■

The above result can be used to compute the tail probability of SINR for $\gamma \geq 1$ for a canonical SCS under certain conditions. We briefly investigate this situation for which we define $\mathcal{L}(f(x), s) \triangleq \int_{x=0}^{\infty}\mathrm{e}^{-sx}f(x)dx$ to be the unilateral Laplace transform of the function $f(x)$.

Lemma 3: A canonical SCS with BS density function $\lambda(r)$ is equivalent to the 1-D SCS with i.i.d. unit-mean exponentially-distributed fading coefficients Ψ_i considered in Lemma 2 if there exists a continuous BS density function $\bar{\lambda}(r) \geq 0$ such that $\mathcal{L}\left(\bar{\lambda}(x), \frac{1}{r}\right)$, $\int_{s=0}^{r}\lambda(s)ds$ exist and

$$\mathcal{L}\left(\bar{\lambda}(x), \frac{1}{r}\right) = \int_{s=0}^{r}\lambda(s)ds, \ \forall\, r \geq 0. \tag{8}$$

As a result, the tail probability of SINR for such canonical SCS is equal to (7).

Proof: The above result is obtained as a consequence of Theorem 2 which says that the two SCSs considered above are equivalent if $\lambda(r) = \mathbb{E}_{\Psi}[\Psi\bar{\lambda}(r\Psi)], \forall\, r \geq 0$, where Ψ is the unity mean exponential random variable representing the fading factors in the latter SCS. By rewriting the expectation in the above equation as an integral and simplifying, we obtain

$$\lambda(r) = \int_{x=0}^{\infty}\frac{d}{dr}\left(\mathrm{e}^{-\frac{x}{r}}\right)\bar{\lambda}(x)dx \stackrel{(a)}{=} \frac{d}{dr}\left(\mathcal{L}\left(\bar{\lambda}(x), \frac{1}{r}\right)\right),$$

where (a) is obtained by exchanging the order of integration and differentiation, which is valid since $\bar{\lambda}(r)$ is continuous. Further, the resultant integral can be written in terms of the Laplace transform of $\bar{\lambda}(x)$. Using $\mathcal{L}\left(\bar{\lambda}(x), \frac{1}{r}\right)\big|_{r=0} = 0$ as the initial condition, the above differential equation can be solved to obtain the condition for equivalence between the two SCSs to be (8). ■

3) Computing Canonical SCS SINR Tail Probabilities From Equivalent SCSs With i.i.d. Rayleigh Fading: The following shows examples for the existence of BS density functions $(\lambda(r), \bar{\lambda}(r))$ that satisfy the condition in (8).

Example 1: Polynomial—polynomial equivalence: The pair $(\lambda(r), \bar{\lambda}(r)) = (\alpha_1 r^{\delta}, \alpha_2 r^{\delta})$ satisfy the condition in (8) as long as $\delta + 1 > 0$, and $\alpha_1 = \alpha_2 \Gamma(1+\delta) > 0$, where $\Gamma(\cdot)$ is the Gamma function.

Example 2: Rational—exponential equivalence: The pair $(\lambda(r), \bar{\lambda}(r)) = \left(\frac{1}{(1+\alpha r)^2}, \mathrm{e}^{-\alpha r}\right), \forall \alpha > 0$ satisfy the condition in (8).

We will see in the following section that the equivalent 1-D BS density function for the homogeneous l-D SCSs are polynomial functions, and using Example 1 and Lemma 2, simple analytical expressions for the tail probability of SINR are obtained.

The results presented in this section can together accurately characterize the SINR in any arbitrary SCS with arbitrary transmission and channel characteristics. The semi-analytical expressions presented above might seem unwieldy at the first glance. But it turns out that several insightful results can be extracted from this representation for a special class of SCSs that are practically important and popular in literature. This special class of SCSs are the homogeneous l-D SCSs, $l \in \{1, 2, 3\}$, and we dedicate the next section to studying this special class in detail.

IV. Homogeneous l-D SCS

In this section, we focus on the analysis of the homogeneous l-D SCSs with a power-law path-loss model $h(R) = R^{\varepsilon}$. The homogeneous l-D SCS is the most widely used stochastic geometric model in the literature for modeling arrangement of node locations. Especially, its validity in the study of the small-cell networks is extremely appealing. Moreover, this model has the advantage of being analytically amenable for a variety of situations that are of great importance in the modeling and analysis of any type of wireless network. The results provide several insights about such large-scale networks that can be applied in the design of actual networks in practice. Next, we apply the results of the previous section to the case of the homogeneous l-D SCS.

Corollary 1. [of Proposition 1]: A homogeneous l-D SCS with a constant BS density λ_0 over the entire space is equivalent to the 1-D SCS with a BS density function $\lambda(r) = \lambda_0 b_l r^{l-1}, \forall r \geq 0$, where $b_1 = 2$, $b_2 = 2\pi$, $b_3 = 4\pi$.

This is easily proved by letting $d(x)$, $d(r,\theta)$, and $d(r,\theta,\phi)$ be λ_0 in Proposition 1.

For the power-law path-loss model $1/h(R) = R^{\varepsilon}$, we have the following equivalent SCS using Corollary 1 and Theorem 2.

Corollary 2. [of Theorem 2]: A homogeneous l-D SCS with BS density λ_0 and path-loss model $\frac{1}{R^{\varepsilon}}$ is equivalent to the 1-D SCS with a BS density function $\bar{\lambda}(r) = \lambda_0 \frac{b_l}{\varepsilon} r^{\frac{l}{\varepsilon}-1}$, $r \geq 0$ and the path-loss model $\frac{1}{R}$.

Next, we characterize the effect of random transmission powers and fading factors, i.i.d. across BSs in the homogeneous l-D SCS. The effect of fading factors with arbitrary distribution on the SINR of homogeneous 2-D SCS has been reported in [18], [29], [30], and the following result generalizes it further.

Corollary 3. [of Theorem 2]: A homogeneous l-D SCS with BS density λ_0, power-law path-loss model $\left(\frac{1}{R^{\varepsilon}}\right)$, random transmission powers and fading factors that have arbitrary joint distribution and are i.i.d. across all the BSs is equivalent to another homogeneous l-D SCS with a BS density $\bar{\lambda} = \lambda_0 \mathbb{E}\left[(K\Psi)^{\frac{l}{\varepsilon}}\right]$, same power-law path-loss model $\left(\frac{1}{R^{\varepsilon}}\right)$, unity transmission power and unity fading factor at each BS, where K, Ψ have the same joint distribution as the transmission power and fading factors of the original homogeneous l-D SCS and $\mathbb{E}[\cdot]$ is the expectation operator w.r.t. K and Ψ, as long as $\mathbb{E}\left[(K\Psi)^{\frac{l}{\varepsilon}}\right] < \infty$.

Proof: Using Corollary 1 and Corollary 2, we obtain a 1-D SCS with BS density function $\tilde{\lambda}(r) = \lambda_0 \frac{b_l}{\varepsilon} r^{\frac{l}{\varepsilon}-1}$, with a path-loss model $\frac{1}{R}$. Now, from Theorem 2, the equivalent canonical SCS has a BS density function $\hat{\lambda}(r) = \mathbb{E}\left[(K\Psi)^{\frac{l}{\varepsilon}}\right] \times \tilde{\lambda}(r)$. This result can be traced back to the scaling of the BS density of the original homogeneous l-D SCS by $\mathbb{E}\left[(K\Psi)^{\frac{l}{\varepsilon}}\right]$. ■

As a result, we can restrict our attention to SINR characterization when all the BSs of the l-D SCS have unity transmission power and fading factors. Now, we give the expression for the tail probability of SINR in a homogeneous l-D SCS.

Corollary 4. [of Theorem 3]: In a homogeneous l-D SCS with a BS density λ_0, unity transmission power and fading factor at each BS, if the path-loss exponent of the power-law path-loss model satisfies $\varepsilon > l$, the characteristic function of the reciprocal of SINR is given by

$$\Phi_{\frac{1}{\mathrm{SINR}}}(\omega) = \mathrm{E}_{R_1}\left[\mathrm{e}^{i\omega\eta R_1} \times \mathrm{e}^{\frac{\lambda_0 b_l}{l} R_1^{\frac{l}{\varepsilon}}\left(1 - {}_1F_1\left(-\frac{l}{\varepsilon}; 1-\frac{l}{\varepsilon}; i\omega\right)\right)}\right], \tag{9}$$

where the p.d.f. of R_1 is $f_{R_1}(r) = \lambda_0 \frac{b_l}{\varepsilon} r^{\frac{l}{\varepsilon}-1} \cdot \mathrm{e}^{-\lambda_0 \frac{b_l}{l} r^{\frac{l}{\varepsilon}}}$, $r \geq 0$. When $\eta = 0$, the SINR is equivalently the signal-to-interference ratio (SIR), and

$$\Phi_{\frac{1}{\mathrm{SIR}}}(\omega) = \frac{1}{{}_1F_1\left(-\frac{l}{\varepsilon}; 1-\frac{l}{\varepsilon}; i\omega\right)}, \tag{10}$$

where ${}_1F_1(\ldots)$ is the confluent hypergeometric function of the first kind [31]. The tail probability of SINR is given by (4).

Proof: From Corollary 2, the SINR distribution is equivalent to the canonical SCS with BS density function $\lambda(r) = \lambda_0 \frac{b_l}{\varepsilon} r^{\frac{l}{\varepsilon}-1}$, $r \geq 0$. Now, by solving for (6), in Theorem 3, we obtain (9). Further, the expectation in (9) reduces to (10). ■

Due to Corollary 3, the homogeneous l-D SCS satisfies the conditions in Lemma 2 and hence a simple expression for the tail probability of SINR for $\gamma \geq 1$ can be derived. A special case of the following result for the homogeneous 2-D SCS and exponential fading case was reported in [32].

Corollary 5. [of Lemma 2]: For a homogeneous l-D SCS with BS density λ_0, path-loss model $\frac{1}{R^\varepsilon}$, $\varepsilon > l$, with unity transmission power and fading factor at each BS, the tail probability of SINR for $\gamma \geq 1$ is

$$\mathbb{P}(\{\mathrm{SINR}>\gamma\}) = \int_{r=0}^{\infty} \frac{\lambda_0 b_l r^{l-1}}{\Gamma\left(1+\frac{l}{\varepsilon}\right)} \exp\left(-\eta\gamma r^{\varepsilon} - \frac{\lambda_0 b_l r^l \pi \gamma^{\frac{l}{\varepsilon}}}{\varepsilon\Gamma\left(1+\frac{l}{\varepsilon}\right)\sin\left(\frac{l\pi}{\varepsilon}\right)}\right) dr, \quad (11)$$

$$= \gamma^{-\frac{l}{\varepsilon}} \mathbb{P}\left(\{\mathrm{SINR} > 1\}\right), \quad (12)$$

and when $\eta = 0$, the tail probability of SIR is

$$\mathbb{P}\left(\{\mathrm{SIR} > \gamma\}\right) = \frac{\sin\left(\frac{l\pi}{\varepsilon}\right)\gamma^{-\frac{l}{\varepsilon}}}{\left(\frac{l\pi}{\varepsilon}\right)} = \mathrm{sinc}\left(\frac{l}{\varepsilon}\right)\gamma^{-\frac{l}{\varepsilon}}. \quad (13)$$

Proof: Due to Corollary 3, the homogeneous l-D SCS is equivalent to another homogeneous l-D SCS with the same path-loss model and transmission powers as the former, and with a BS density $\frac{\lambda_0}{\Gamma\left(1+\frac{l}{\varepsilon}\right)}$ and i.i.d. unity mean exponential random fading factors at each BS. Using Corollary 2, the BS density function of the 1-D SCS with $\frac{1}{R}$ path-loss model that is equivalent to the latter homogeneous l-D SCS is $\bar{\lambda}(r) = \frac{\lambda_0 b_l r^{\frac{l}{\varepsilon}-1}}{\varepsilon\Gamma\left(1+\frac{l}{\varepsilon}\right)}$, $r \geq 0$. An alternate approach to obtain the expression for $\bar{\lambda}(r)$ is using Lemma 3 and Example 1.

For the 1-D SCS, Lemma 2 is used to obtain the expression for the tail probability of SINR to be (11), using the identity $\int_{s=0}^{\infty} \frac{s^{\frac{l}{\varepsilon}-1} ds}{1+(\gamma r)^{-1}s} = \frac{\pi(\gamma r)^{\frac{l}{\varepsilon}}}{\sin\left(\frac{l\pi}{\varepsilon}\right)}$. Finally, (12) and (13) are obtained by simple change of variables. This completes the proof. ■

Using Corollaries 4 and 5, the expression for the tail probability of SINR in a homogeneous l-D SCS with random transmission power and fading factor with an arbitrary joint distribution that are i.i.d. across the BSs of the SCS can be obtained by merely scaling the BS density λ_0 with an appropriate constant that is given in Corollary 3.

The following lemma shows another interesting property of the SINR distribution in a homogeneous l-D SCS.

Lemma 4: The SINR distribution in a homogeneous l-D SCS with a constant BS density λ_0, path-loss model $\frac{1}{R^\varepsilon}$, unity transmission power and fading factor at each BS with a background noise power η is the same as in a homogeneous l-D SCS with the same path-loss model, unity BS density, unity transmission power and fading factor at each BS and a background noise power $\eta\lambda_0^{-\frac{\varepsilon}{l}}$. Equivalently,

$$\mathrm{SINR}(\lambda_0, \varepsilon, \eta) =_{\mathrm{st}} \mathrm{SINR}\left(1, \varepsilon, \eta\lambda_0^{-\frac{\varepsilon}{l}}\right). \quad (14)$$

Proof: $\mathrm{SINR}(\lambda_0, \varepsilon, \eta) = \left.\frac{R_1^{-\varepsilon}}{\sum_{k=2}^{\infty} R_k^{-\varepsilon}+\eta}\right|_{\lambda_l(r)} \overset{(a)}{=}_{\mathrm{st}} \left.\frac{(\alpha R_1)^{-\varepsilon}}{\sum_{i=2}^{\infty}(\alpha R_i)^{-\varepsilon}+\eta\alpha^{-\varepsilon}}\right|_{\lambda_l(r)} \overset{(b)}{=}_{\mathrm{st}} \left.\frac{(R_1')^{-\varepsilon}}{\sum_{k=2}^{\infty}(R_k')^{-\varepsilon}+\bar{\eta}}\right|_{\frac{1}{\alpha}\lambda_l\left(\frac{r}{\alpha}\right)}$, where $\alpha = \lambda_0^{\frac{1}{l}}$; $\bar{\eta} = \eta\alpha^{-\varepsilon}$; (a) is obtained by expressing SINR in terms of the equivalent 1-D SCS with $\lambda_l(r) = \lambda_0 b_l r^{l-1}$, $r \geq 0$, and multiplying numerator and denominator with $\alpha^{-\varepsilon}$; (b) follows from Corollary 1; and finally, (14) is obtained by noting that the 1-D SCS with BS density function $\frac{1}{\alpha}\lambda_l\left(\frac{r}{\alpha}\right)$ in (b) corresponds to a homogeneous l-D SCS with BS density 1. ■

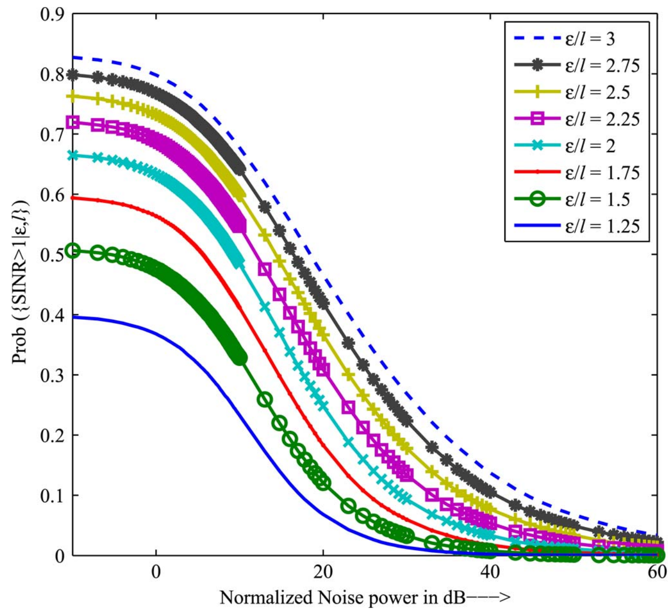

Fig. 2. Plot of Prob($\{\mathrm{SINR} > 1\}$) vs normalized noise power, $\eta\lambda^{-\frac{\varepsilon}{l}}$, for a homogeneous l-D SCS

Therefore, it is sufficient to analyze a *homogeneous* l-D SCS with BS density $\lambda_0 = 1$ and maintain a lookup table for the tail probability of SINR for different values of the noise powers and path-loss exponents using (4). The lookup table is presented for a *homogeneous* 2-D SCS in Fig. 2 as a plot of $\mathbb{P}(\{\mathrm{SINR} > 1\})$ against noise powers for different values of path-loss exponents, which with (12) completely characterizes the tail probability for $\gamma \geq 1$. Further, in a *homogeneous* l-D SCS with a high BS density λ_0, the equivalent noise power $\eta\lambda_0^{-\frac{\varepsilon}{l}}$ is small according to Lemma 4. Hence, in an *interference-limited system* (large λ_0), the signal quality can be measured in terms of SIR. Further remarks on SIR of a homogeneous l-D SCS based on Corollaries 4 are given below.

Remark 1: The characteristic function of the $\frac{1}{\mathrm{SIR}}$ does not depend on λ_0, and hence the tail probability of SIR at a MS in a homogeneous l-D SCS does not depend on λ_0.

Remark 2: From Corollary 1 and Remark 1, the tail probability of SIR is invariant to random transmission powers and fading factors with arbitrary joint distribution and i.i.d. across the BSs.

Remark 3: The expression for the characteristic function of $\frac{1}{\mathrm{SIR}}$ for a *homogeneous* 2-D and 3-D SCS is same as that of a *homogeneous* 1-D SCS with path-loss exponents $\frac{\varepsilon}{2}$ and $\frac{\varepsilon}{3}$, respectively.

Remark 3 helps build an intuition of why the *homogeneous* 1-D SCS has a higher tail probability of SIR than *homogeneous* 2-D and 3-D SCSs. As the path-loss exponent decreases, the BSs farther away from the MS have a greater contribution to the total interference power at the MS, and this leads to a poorer SIR at the MS and a smaller tail probability. Next, Fig. 3(a) shows the tail probabilities of SIR in a *homogeneous* 2-D SCS as a function of the path-loss exponent ε; the squares ($\square$)

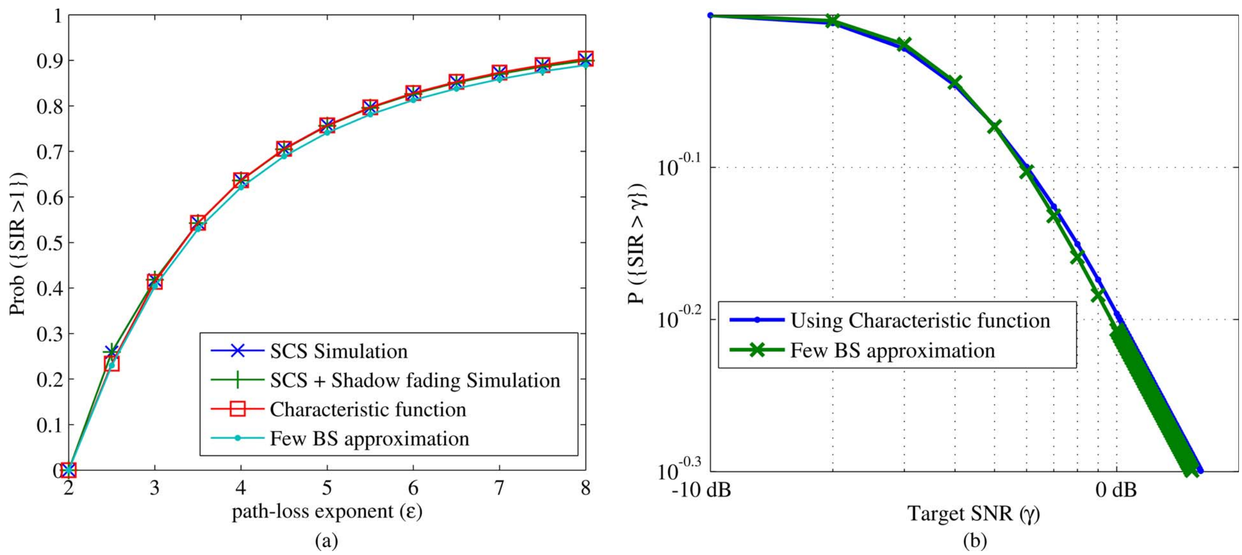

Fig. 3. (a) Comparison of Simulations with the analytical results for a homogeneous 2-D SCS. (b) Comparing exact SIR and the few BS approximation for path-loss $\varepsilon = 4$.

and the pluses $(+)$ represent the values computed analytically and by Monte-Carlo simulations, respectively. According to Remark 3, the same figure can be used for 1-D and 3-D systems with path-loss exponent ε' using the scaling $\varepsilon = 2\varepsilon'$ and $\varepsilon = \frac{2}{3}\varepsilon'$.

In the following, we present an approximation to SIR based on modeling the interference due to the strongest few BSs accurately and the interference due to the rest by their ensemble average. The approximation is expected to be tight for low BS densities. Due to Remark 1, the same approximation will be tight for all BS densities. Now, we define the so-called *few BS approximation* and derive closed form expressions for the tail probability of SIR at MS in a *homogeneous* l-D SCS for both the SIR regions [0,1) and $[1, \infty)$.

Definition 4: The few BS approximation corresponds to modeling the total interference power at the MS in a SCS as the sum of the contributions from the strongest few interfering BSs and an ensemble average of the contributions of the rest of the interfering BSs.

Recall that the total interference power is $P_I = \sum_{i=2}^{\infty} R_i^{-\varepsilon}$, where $\{R_i\}_{i=1}^{\infty}$ is the set of distances of BSs arranged in the ascending order of their separation from the MS. The arrangement also corresponds to the descending order of their contribution to P_I, due to path-loss. In the few BS approximation, P_I is approximated by $\tilde{P}_I(k) = \sum_{i=2}^{k} R_i^{-\varepsilon} + \mathbb{E}[\sum_{i=k+1}^{\infty} R_i^{-\varepsilon}|R_k]$, for some k, where $\mathbb{E}[\cdot]$ is the expectation operator and corresponds to the ensemble average of the contributions of BSs beyond R_k. The SIR at the MS obtained by the few BS approximation is denoted by SIR_k. The expectation is calculated as follows.

Lemma 5: For a homogeneous l-D SCS, with BS density λ_0 and $\varepsilon > l$, for $k = 1, 2, 3, \cdots$,

$$\mathbb{E}\left[\sum_{i=k+1}^{\infty} R_i^{-\varepsilon}\middle| R_k\right] = \frac{\lambda_0 b_l R_k^{l-\varepsilon}}{\varepsilon - l}. \tag{15}$$

Proof: Firstly, use Corollary 1 to reduce the l-D SCS to an equivalent 1-D SCS with BS density function $\lambda(r) = \lambda_0 b_l r^{l-1}$, $\forall\, r \geq 0$. Next, given k, using the Superposition theorem of Poisson processes, the original Poisson process is equivalent to the union of two independent Poisson processes defined in the non-overlapping regions $[0, R_k]$ and $(R_k,\, \infty)$, respectively, with the same BS density function. Now, using Campbell's theorem [1, (3.18), p. 28] to the Poisson process defined in (R_k, ∞), we obtain (15). ■

The following theorem gives the SIR tail probability approximation, using $k = 2$.

Theorem 4: In a homogeneous l-D SCS with BS density λ_0 and path-loss exponent ε, satisfying $\varepsilon > l$, the tail probability of SIR_2 at the MS is given by

$$\mathbb{P}(\{\mathrm{SIR}_2 > \gamma\}) = \begin{cases} \gamma^{-\frac{l}{\varepsilon}} C_{\frac{\varepsilon}{l}}, & \gamma \geq 1 \\ 1 - e^{-u(\gamma)}\left(1 + u(\gamma)\right) + \gamma^{-\frac{l}{\varepsilon}} D_{\frac{\varepsilon}{l}}(\gamma), & \gamma < 1, \end{cases} \tag{16}$$

where $C_{\frac{\varepsilon}{l}} = G(0)$ and $D_{\frac{\varepsilon}{l}}(\gamma) = G(u(\gamma))$ with $G(a) = \int_{v=a}^{\infty} \frac{v e^{-v}}{\left(1+v\left(\frac{\varepsilon}{l}-1\right)^{-1}\right)^{\frac{l}{\varepsilon}}} dv$, and $u(\gamma) \equiv \left(\frac{\varepsilon}{l} - 1\right)\left(\frac{1}{\gamma} - 1\right)$.

Proof: See Appendix F. ■

The above approximation can be further tightened by recalling that we already have a simple closed-form expression in (13) for the tail probability of SIR for values in the range $[1, \infty)$. Hence, the new approximation is as follows

$$\mathbb{P}(\{\mathrm{SIR}_{approx} > \gamma\}) = \begin{cases} \mathbb{P}(\{\mathrm{SIR} > \gamma\}) & ,\gamma \geq 1 \\ \mathbb{P}(\{\mathrm{SIR}_2 > \gamma\}) & ,\gamma < 1, \end{cases} \tag{17}$$

where the relevant quantities are obtained from (13) and Theorem 4.

Notice that $\mathbb{P}(\{\mathrm{SIR} > \gamma\}) = \frac{\mathrm{sinc}\left(\frac{l}{\varepsilon}\right)}{C_{\frac{\varepsilon}{l}}} \mathbb{P}(\{\mathrm{SIR}_2 > \gamma\})$ for $\gamma \geq 1$. Fig. 3(a) shows that the few BS approximation (•) closely follows the actual behavior (□). Fig. 3(b) shows the comparison of the tail probabilities of SIR (computed using Corollaries 4 and 5) and SIR_2 for a *homogeneous* 2-D SCS with path-loss exponent 4. Notice that the gap between the two tail probability curves is negligible in the region $\gamma \in [0, 1]$, and further, both the curves are straight lines parallel to each other

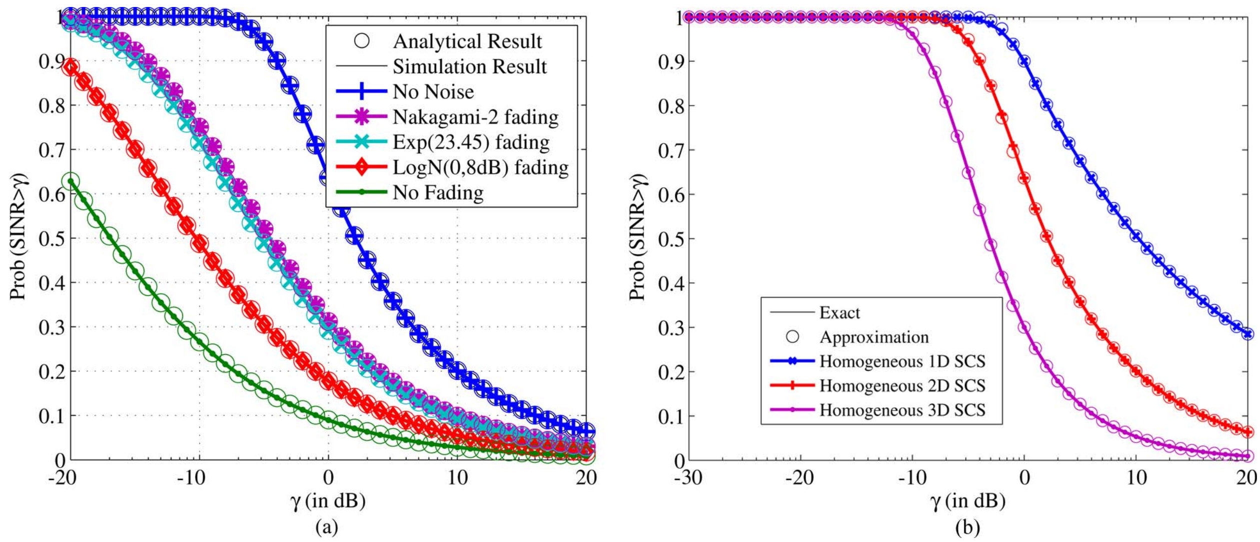

Fig. 4. (a) Comparing the SINR distributions for various fading distributions and noise profiles (Nakagami-2 refers to the Nakagami distribution with a shape parameter 2 and mean 23.45, Exp(23.45) refers to an exponential random variable with mean 23.45, logN(0,8 dB) refers to a log-normal random variable whose natural logarithm has a mean and variance of 0 and 8 dB, respectively). (b) Evaluating the tightness of the few-BS approximation.

in the region $\gamma \in [1, \infty)$, when the tail probability is plotted against γ, both in the logarithmic scale. This shows that the few BS approximation characterizes the signal quality in closed form and is a good approximation for the actual SIR.

Now, having characterized the SIR for the homogeneous l-D SCS, we look closely into what happens when $\varepsilon \leq l$. We will restrict ourselves to the case when $l = 2$, and the steps are similar for $l = 1$, and $l = 3$.

Theorem 5: A homogeneous 2-D SCS with BS density λ, where the signal decays according to a power-law path-loss function with a path-loss exponent $\varepsilon \leq 2$, the SIR at the MS is 0 with probability 1.

Proof: See Appendix G for the case $\varepsilon = 2$. From [17, Corollary 5], $\mathbb{P}(\{\text{SIR} > \gamma\})|_{\varepsilon<2} \leq \mathbb{P}(\{\text{SIR} > \gamma\})|_{\varepsilon=2} = 0, \forall\gamma \geq 0$. Hence we have proved the above result. ■

Note that once we have characterized the SINR distribution, the outage probability at the MS is known. The event that the MS is in coverage is given by $\{\text{SINR} > \gamma\}$, where γ is the SINR threshold that the MS should satisfy to be in coverage. Consequently, the coverage probability, $\mathbb{P}(\{\text{SINR} > \gamma\})$ is precisely the tail probability of SINR computed at γ. Next, we study the area-averaged spectral efficiency [33, Page 77] for an MS in coverage. This quantity, termed as the coverage conditional average rate, is given by $\mathcal{R} = \mathbb{E}[\log(1 + \text{SINR})|\{\text{SINR} > \gamma\}]$ and is the average of the instantaneous rate achievable at the MS when the interference is considered as noise. The coverage conditional average rate at the MS simplifies to the following expression.

$$\mathcal{R} = \log(1+\gamma) + \int_{t=\gamma}^{\infty} \frac{\mathbb{P}\left(\{\text{SINR} > t\}\right)}{(1+t)\mathbb{P}\left(\{\text{SINR} > \gamma\}\right)} dt.$$

As a result, based on Proposition 1 and Theorems 1-2, we can compute the coverage conditional average rate for any SCS. Specifically, in the interference-limited case, the following proposition provides the expression for a homogeneous l-D SCS and when the popular power-law path-loss model is assumed. For this case, the SIR characteristics are invariant to the randomness in the transmission powers and the fading factors due to Remark 2. Hence, without loss of generality, we restrict our attention to the case of constant transmission powers at all BSs and no fading.

Proposition 2: The ergodic average rate at the MS in a homogeneous 2-D SCS under the power-law path-loss model, with constant transmission powers at all BSs and no fading is given by

$$\mathcal{R} = \log(1+\gamma) + \int_{x=\gamma}^{\alpha} \frac{\mathbb{P}\left(\{\text{SIR} > x\}\right)}{\mathbb{P}\left(\{\text{SIR} > \gamma\}\right)(1+x)} dx + \alpha^{-\frac{2}{\varepsilon}} \frac{\varepsilon}{2} \cdot {}_2F_1\left(1, \frac{2}{\varepsilon}; 1 + \frac{2}{\varepsilon}; -\alpha^{-1}\right),$$

where $\alpha = \max(\gamma, 1)$, where ${}_2F_1\left(1, \frac{2}{\varepsilon}; 1 + \frac{2}{\varepsilon}; -\alpha^{-1}\right)$ is the Gauss hypergeometric function and the probabilities are computed using (4). Note that for $\gamma \geq 1$, the middle term drops out.

V. Numerical Example and Discussion

In the first example, we consider a homogeneous 2-D SCS with $\lambda = 0.01$, a power-law path-loss model with path-loss exponent 4, and a background noise power of -10 dB and unity transmission powers. We compare the SINR tail probabilities for several cases where we vary the distributions of the fading factors as well as the background noise power. Notice in Fig. 4(a) that in the case when there is background noise, the distribution of the fading greatly affects the SINR performance at the MS. We consider three examples for the i.i.d. fading factors: Nakagami distribution with a shape parameter 2, exponential distribution and log-normal distribution, and keep the same mean (=23.45) for all the cases, for a fair comparison. In the presence of the background noise, the MS sees a better SINR performance for the Nakagami and the exponential case compared to the log-normal case and the SINR performance in all cases is far more superior than that without fading. This is justified by Corollary 3 and Lemma 4 where the equivalent homogeneous 2-D SCS with unity BS density has an equivalent background noise power for the log-normal fading case that is strictly greater than that for the exponential fading and the Nakagami distributions. Further, in the no noise case, the SINR performance is invariant to the fading distribution and is the same as in the no fading case. This is also depicted in Fig. 4(a).

In Fig. 4(b), we assess the few-BS approximation for the SIR characterization in the homogeneous l-D SCS. This figure shows that the SIR approximation derived in Section IV based on the few-BS approximation (Equation (17)) closely follows the exact SIR characterization. Moreover, this relationship holds for a wide range of scenarios of interest such as for arbitrary fading and transmission power distributions, and for all BS densities. In the following section, we discuss the usage of the results obtained thus far in the analysis of other useful wireless communication scenarios.

VI. Applications in Wireless Communications

We discuss several scenarios where the wireless communication systems are modeled by the *homogeneous* l-D SCS with BS density λ_0, where $l = 1, 2$, and 3 correspond to highway, suburban, and dense urban deployments, respectively.

BSs With Sectorized Antennas: In this example, we give a practical scenario where the transmission powers of the BSs are i.i.d. random variables. For example, consider the case where each BS has an ideal sectorized antenna with gain G and beamwidth θ, such that BS's antenna faces the MS with probability $\frac{\theta}{2\pi}$, in which case $K_i = G$, and otherwise $K_i = 0$. In this case, in the absence of fading, from Corollary 3, $\overline{\lambda}_0 = \lambda_0 G^{\frac{2}{\varepsilon}} \frac{\theta}{2\pi}$ is the BS density of the equivalent *homogeneous* l-D SCS.

Multiple Access Techniques: Next, we study the signal quality at the MS in a cellular system employing different multiple access techniques. For example, in a code division multiple access (CDMA) system, the goal is to maintain a constant voice signal quality at the MS, which is done by power control. This goal is achievable by having the serving BS increase its transmission power by $\alpha = \gamma \mathrm{SIR}^{-1}$, where α is the power control factor or the processing gain, SIR is the instantaneous signal quality at the MS, and γ is the desired constant signal quality. In this formulation, α for each BS is a random variable and in general, the α's of nearby BSs are correlated. But if the correlation is small, the SIR distribution computed here enables radio designers to approximately model the power needs to communicate with a MS in a SCS. In another formulation, if α is a constant factor by which the power of the serving BS is improved, its effect on the tail probability SIR at the MS is obtained by straightforward manipulations as $\mathbb{P}(\{\alpha \times \mathrm{SIR} > \gamma|\varepsilon, l\}) = \mathrm{sinc}\left(\frac{l}{\varepsilon}\right)\left(\frac{\gamma}{\alpha}\right)^{-\frac{l}{\varepsilon}}$ if $\gamma > \alpha$.

Then, consider frequency division multiple access (FDMA) and time division multiple access (TDMA) based cellular systems. Let the available spectrum (in frequency for FDMA and in time-slots for TDMA) be divided into N channel reuse groups (CG), and indexed as $k = 1, 2, \cdots, N$. Then, each BS is assigned one of the N CGs, such that the k^{th} CG is assigned with probability p_k. In such a system, the MS chooses a CG that corresponds to the best SIR; the BS in the CG that corresponds to the strongest received power is the *desired* BS, and the MS chooses it as the serving BS. The SIR at the MS in such a SCS is of interest to us. Note that this *homogeneous* l-D SCS is equivalent to N independent *homogeneous* l-D SCSs with constant BS densities $\lambda_0 p_1, \cdots, \lambda_0 p_N$, by the properties of Poisson point processes. The tail probability of SIR at the MS in such a system is given by $\mathbb{P}(\{\mathrm{SIR} > \gamma|\varepsilon, N\}) = 1 - [1 - \mathbb{P}(\{\mathrm{SIR} > \gamma|\varepsilon\})]^N$, where the tail probability on the right hand side is computed using Corollary 4.

Cognitive Radios: In cognitive radio technology, the cognitive radio devices (or *secondary users*) opportunistically operate in licensed frequency bands occupied by *primary users*. The interference caused by *secondary user* transmissions is harmful for *primary users* operation, and is not acceptable beyond certain limits. Studying the nature of these interferences and formulating methods for addressing them has been an active area of research (see [34]–[37]). Although the interference study of the cognitive radio networks needs more complicated stochastic geometric models, a Poisson point process models several useful scenarios. The general results in this paper are a rich source of mathematical tools for studying these scenarios. In [19], [38], we have extensively applied the ideas and results developed here to understand the role of cooperation between the *secondary users* in ensuring that the interference caused by the *secondary users* are within the acceptable limits. The *secondary users* are modeled analogous to BS placement in *homogeneous* 1-D and 2-D SCS, and the tail probability of $\frac{C}{I}$ at the *primary user* is characterized. Further, in the context of radio environment map (REM, [19, and references therein]), we have highlighted the practical significance of the study of 1-D SCS.

Overlay Networks: The modern cellular communication network is a complex overlay of heterogeneous networks, such as macrocells, microcells, picocells and femtocells. This complex overlay network is seldom studied as is since the correlation between the node locations and fading factors in such dense networks tend to make performance studies analytically intractable. Yet, simpler cases where the node locations as well as the fading factors are independent are well modeled by Poisson point processes, and provide interesting insights about such networks. In [39], [40], cellular systems consisting of macrocell and femtocell networks are analyzed. Using the results in our paper, the cumulative effect of all the networks constituting the overlay network, on the signal quality at the MS can be studied. A detailed study on this is set aside as a future work, while the preliminary results are presented in [16], [18], [41]. Other efforts on the downlink performance characterization for heterogeneous networks can be found in [22], [32], [42]–[47].

VII. Conclusion

In this paper, we study the characterization of the SIR and SINR at the MS in shotgun cellular systems where a SCS is defined as a cellular system where the BS deployment in a given region is according to a Poisson point process. A sequence of equivalent SCSs are derived to show that it is sufficient to study the canonical SCS that has unity transmission power and unity fading factors, and a path-loss model of $\frac{1}{R}$. Analytical expressions for the tail probabilities of the SIR and SINR at the MS are obtained for 1-D, 2-D, and 3-D SCSs, where the 1-D, 2-D, and 3-D SCS are mathematical models for BS deployments along the highway (1-D), in planar regions (2-D) and in urban areas (3-D), respectively. Further, a closed form expression for the tail probability of SIR is derived for the homogeneous cases of 1-D, 2-D, and 3-D SCS. The results are applicable for general fading distributions and arbitrary path-loss models. This makes the results useful for analyzing many different wireless scenarios that are characterized by uncoordinated deployments. The application of the results has been demonstrated in the study of the impact of cooperation between cognitive radios in the low power primary user detection and can be found in [19], and in the study of heterogeneous networks in [18]. Future work will further explore the applications of the SCS model in the context of indoor femtocells, cognitive radios, and multi-tier or overlay networks.

APPENDIX

A. Proof for Path-loss Equivalence Theorem (Theorem 1)

Let $\bar{R} = h(R)$ be the equivalent BS location. Using the *Mapping Theorem* in [1], BS with locations $\bar{R}$ is also a Poisson point process, whose density is obtained below. For any non-homogeneous 1-D Poisson point process, $\mathbb{E}[N(r+s) - N(r)] = \int_r^{r+s} \lambda(z)dz$ is the expected number of occurrences in the interval $(r, r+s)$. Thus,

$$\begin{aligned}
&\mathbb{E}\left[N(r+s) - N(r)\right] \\
&= \mathbb{E}\left[\text{Number of BSs with } \bar{R} \in (r, r+s)\right] \\
&= \mathbb{E}\left[\text{Number of BSs with } R \in \left(h^{-1}(r), h^{-1}(r+s)\right)\right] \\
&= \int_{z=h^{-1}(r)}^{h^{-1}(r+s)} \lambda(z)dz = \int_{z=r}^{r+s} \frac{\lambda\left(h^{-1}(z)\right)}{h'\left(h^{-1}(z)\right)} dz. \qquad (18)
\end{aligned}$$

Hence, the 1-D SCS with path-loss model $\frac{1}{h(R)}$ and a BS density function $\lambda(r)$ is equivalent to the 1-D SCS with path-loss model $\frac{1}{R}$ and BS density function $\bar{\lambda}(r)$.

B. Proof for Arbitrary Fading Equivalence Theorem (Theorem 2)

Let $\bar{R} = R(K\Psi)^{-1}$, where R is the random variable representing the distance from the MS to a BS in the 1-D SCS with a BS density function $\lambda(r)$, K, Ψ are the transmission power and the fading factor corresponding to the BS, respectively, and $\bar{R}$ is the corresponding equivalent distance. Using the *product space representation* and *Marking Theorem* in [1], $\bar{R}$ also corresponds to the 1-D SCS with a BS density function derived following (18):

$$\begin{aligned}
\mathbb{E}\left[N(r+s) - N(r)\right] &\overset{(a)}{=} \mathbb{E}_{K,\Psi}\left[\int_{rK\Psi}^{(r+s)K\Psi} \lambda(z)dz\right] \\
&\overset{(b)}{=} \int_r^{(r+s)} \mathbb{E}_{K,\Psi}\left[K\Psi\lambda(K\Psi z)\right]dz,
\end{aligned}$$

where (a) is obtained by rewriting the expectation with respect to each realization of Ψ and K, and (b) is obtained by exchanging the order of integration and expectation in (b) as $\mathbb{E}_{K,\Psi}[K\Psi\lambda(K\Psi z)] < \infty$. Hence, $\bar{R}'s$ corresponds to the 1-D SCS with a BS density function $\bar{\lambda}(r) = \mathbb{E}_{K,\Psi}[K\Psi\lambda(K\Psi r)]$.

C. Proof for Lemma 1

Let $\{R_k\}_{k=1}^{\infty}$ correspond to the 1-D SCS with BS density function $\lambda(r)$. Then, since the ordered base station locations R_k's are determined by inter-base station distances, it follows that $\text{SINR}|_{\lambda(r)} \overset{(i)}{=} \left.\frac{(aR_1)^{-1}}{\sum_{k=2}^{\infty}(aR_k)^{-1} + \frac{\eta}{a}}\right|_{\lambda(r)} \overset{(ii)}{=}_{\text{st}} \left.\frac{\left(R_1'\right)^{-1}}{\sum_{k=2}^{\infty}(R_k')^{-1} + \frac{\eta}{a}}\right|_{\frac{1}{a}\lambda\left(\frac{r}{a}\right)}$, where the SINR expression is obtained using (2) with $h(R) = R$, (i) is obtained by multiplying the numerator and denominator by $\frac{1}{a}$, $a > 0$; (ii) is because $\{R_k'\}_{k=1}^{\infty}$ can be shown to correspond to 1-D SCS with BS density $\frac{1}{a}\lambda\left(\frac{r}{a}\right)$, $a > 0$, due to Theorem 1. By substituting $\eta = 0$, it is clear that the SIR distributions of all the canonical 1-D SCSs with the BS density functions of the form $\frac{1}{a}\lambda\left(\frac{r}{a}\right)$, $a > 0$ are equivalent.

D. Proof for the Tail Probability of SINR (Theorem 3)

The following are the sequence of step to derive the expression in (4).

$$\begin{aligned}
&\mathbb{P}\left(\{\text{SINR}_{\text{canonical}} > \gamma\}\right) \\
&= \mathbb{P}\left(\left\{\frac{1}{\text{SINR}_{\text{canonical}}} < \frac{1}{\gamma}\right\}\right) \\
&\overset{(a)}{=} \int_{x=0}^{\frac{1}{\gamma}} \int_{\omega=-\infty}^{\infty} \Phi_{\frac{1}{\text{SINR}_{\text{canonical}}}}(\omega) \mathrm{e}^{-i\omega x} \frac{d\omega}{2\pi} dx,
\end{aligned}$$

where (a) is obtained by rewriting the c.d.f. of $\frac{1}{\text{SINR}_{\text{canonical}}}$ in terms of the characteristic function of $\frac{1}{\text{SINR}_{\text{canonical}}}$, where the inner integration computes the p.d.f. of $\frac{1}{\text{SINR}_{\text{canonical}}}$, and the outer integration gives the c.d.f. at $\frac{1}{\gamma}$. When $\gamma = 0$, the above event occurs with probability 1, and otherwise, it is expressed in terms of the integration in (4) which is obtained by exchanging the order of integrations in (a), which is valid in this case, and then evaluating the integral w.r.t. x. In the rest of this section, we derive the expression for $\Phi_{\frac{1}{\text{SINR}_{\text{canonical}}}}(\omega)$, by first noting that $\text{SINR}_{\text{canonical}} = \frac{R_1^{-1}}{\sum_{k=2}^{\infty} R_k^{-1} + \eta}$.

$$\begin{aligned}
\Phi_{\frac{1}{\text{SINR}_{\text{canonical}}}}(\omega) &\overset{(a)}{=} \mathbb{E}_{R_1}\left[\Phi_{\frac{1}{\text{SINR}_{\text{canonical}}}|R_1}(\omega|\, R_1)\right] \\
&\overset{(b)}{=} \mathbb{E}_{R_1}\left[\mathrm{e}^{i\omega\eta R_1} \Phi_{\left.\frac{\sum_{k=2}^{\infty} R_k^{-1}}{R_1^{-1}}\right|R_1}(\omega|\, R_1)\right] \\
&= \mathbb{E}_{R_1}\left[\mathrm{e}^{i\omega\eta R_1} \Phi_{\sum_{k=2}^{\infty} R_k^{-1}|R_1}(\omega R_1|\, R_1)\right] \\
&\overset{(c)}{=} \mathbb{E}_{R_1}\left[\mathrm{e}^{i\omega\eta R_1} \mathbb{E}\left[\left.\prod_{k=2}^{\infty} \mathrm{e}^{i\omega R_1 R_k^{-1}}\right| R_1\right]\right] \\
&\overset{(d)}{=} \mathbb{E}_{R_1}\left[\mathrm{e}^{i\omega\eta R_1} \cdot \exp\left(-\int_{r=R_1}^{\infty} \left(1 - \mathrm{e}^{i\omega R_1 r^{-1}}\right)\lambda(r)dr\right)\right],
\end{aligned}$$

where (a) is obtained due to the properties of expectation, and R_1 is the random variable for the distance of the closest BS from the origin; (b) is obtained by using the properties of the characteristic functions and noting that in $\frac{1}{\text{SINR}_{\text{canonical}}} = \frac{\sum_{k=2}^{\infty} R_k^{-1} + \eta}{R_1^{-1}}$, conditioned on R_1, the term $\frac{\eta}{R_1^{-1}}$ is a constant and hence separates out as $\mathrm{e}^{i\omega\eta R_1}$ from the original conditional characteristic function expression in (a); (c) is obtained by rewriting the exponential of summation in the characteristic function term in (b) as a product of exponentials; (d) is obtained by first noting that conditioned on R_1, the events in the two disjoint regions $[0, R_1]$ and (R_1, ∞) are independent of each other, and hence by the Restriction theorem [1, Page 17], all the points beyond R_1, represented by the set $\{R_k\}_{k=1}^{\infty}$ can be regarded to be associated with a Poisson point process in 1-D restricted to the region (R_1, ∞), and with a density function $\lambda(r)$. As a result, now we can apply Campbell's theorem [1, (3.18), p. 28] to the inner expectation in (c) to obtain (d), which is further simplified to obtain (6).

E. Proof for Lemma 2

Here, we derive the expression for the tail probability of SINR for values greater than or equal to 1. Due to [32, Lemma 1], there exists a unique BS within the 1-D SCS such that $\gamma \geq 1$ holds true. Suppose the index of this unique BS is i. Then the expression for the tail probability of SINR_i, the SINR at the user when receiving from this BS, is given by

$$\begin{aligned}
&\mathbb{P}\left(\{\mathrm{SINR}_i > \gamma\}\right) \\
&\overset{(a)}{=} \mathbb{P}\left(\left\{\frac{\Psi_i R_i^{-1}}{\sum_{j=1,\, j\neq i}^{\infty} \Psi_j R_j^{-1} + \eta} > \gamma\right\}\right) \\
&\overset{(b)}{=} \mathbb{E}\left[\exp(-\eta\gamma R_i) \prod_{j=1, j\neq i}^{\infty} \exp\left(-\gamma R_i \Psi_j R_j^{-1}\right)\right] \\
&\overset{(c)}{=} \mathbb{E}\left[\exp(-\eta\gamma R_i)\times\right. \\
&\left.\exp\left(-\int_{r=0}^{\infty}\left(1-\mathbb{E}_{\Psi}\left[\mathrm{e}^{-\gamma R_i \Psi r^{-1}}\right]\right)\bar{\lambda}(r)dr\right)\right] \\
&\overset{(d)}{=} \mathbb{E}\left[\exp(-\eta\gamma R_i)\times\right. \\
&\left.\exp\left(-\int_{r=0}^{\infty}\left(1-\frac{1}{1+\gamma R_i r^{-1}}\right)\bar{\lambda}(r)dr\right)\right],
\end{aligned}$$

where (a) is the expression for the tail probability of SINR of the 1-D SCS with BS density $\bar{\lambda}(r)$ for which $\{R_j\}_{j=1}^{\infty}$ is the set of distances of BSs from the MS and 'i' is the index of the unique BS that can satisfy the constraint $\{\mathrm{SINR} > \gamma\}$; (b) is obtained by evaluating the expectation w.r.t. Ψ_i and the expectation operator $\mathbb{E}$ is w.r.t. to all other random variables in (a); (c) is obtained by first conditioning w.r.t. R_i and by Slivnyak's theorem noting that the Palm distribution (see [21, Chapter 8] and [3, Chapter 13] for details on Palm theory and Slivnyak's theorem) of the BSs represented by $\{R_j\}_{j=1,j\neq i}^{\infty}$ given a BS at R_i is still a Poisson point process with density function $\bar{\lambda}(r)$, then applying the Marking theorem [1, Page 55] and Campbell's theorem [1, (3.18), p. 28] where Ψ is the unity mean exponential random variable; (d) is obtained by evaluating the expectation in (c); and finally, since there is a unique BS i such that $\mathrm{SINR}_i \geq 1$, we can write the tail probability of SINR as $\mathbb{P}(\{\mathrm{SINR} > \gamma\}) = \mathbb{P}(\cup_{i=1}^{\infty}\{\mathrm{SINR}_i > \gamma\}) = \sum_{i=1}^{\infty}\mathbb{P}(\{\mathrm{SINR}_i > \gamma\})$ $\mathbb{E}\left[\sum_{i=1}^{\infty}\exp(-\eta\gamma R_i)\exp\left(-\int_{s=0}^{\infty}\frac{\bar{\lambda}(s)ds}{1+(\gamma R_i)^{-1}s}\right)\right]$ (from (d)) $=$ (7) from Campbell's Theorem [1, (3.18), p. 28].

F. Proof for the Few-BS Approximation Theorem (Theorem 4)

First, using Corollary 5, $\mathrm{SIR}_2 = \frac{K R_1^{-\varepsilon}}{\tilde{P}_I(2)}$, with $\tilde{P}_I(2) = K R_2^{-\varepsilon}\left(1+\frac{\lambda_0 b_l}{\varepsilon - l}R_2^l\right)$. Next, notice that the event $\{\mathrm{SIR}_2 > \gamma\}$ is equivalent to the joint event $\left\{R_1 \leq R_2, R_1 < \left(\frac{\gamma\tilde{P}_I(2)}{K}\right)^{-\frac{1}{\varepsilon}}\right\}$ and thus, $\mathbb{P}(\{\mathrm{SIR}_2 > \gamma\}) = \mathbb{P}\left(\left\{R_1 \leq \min\left(R_2, \left(\frac{\gamma\tilde{P}_I(2)}{K}\right)^{-\frac{1}{\varepsilon}}\right)\right\}\right)$, where

$$\min\left(R_2, \left(\frac{\gamma\tilde{P}_I(2)}{K}\right)^{-\frac{1}{\varepsilon}}\right) = \begin{cases} \left(\frac{\gamma\tilde{P}_I(2)}{K}\right)^{-\frac{1}{\varepsilon}}, & \gamma \geq 1 \\ \left(\frac{\gamma\tilde{P}_I(2)}{K}\right)^{-\frac{1}{\varepsilon}}, & \gamma < 1, R_2 > \left(\frac{l\times u(\gamma)}{\lambda_0 b_l}\right)^{\frac{1}{l}} \\ R_2, & \gamma < 1, R_2 \leq \left(\frac{l\times u(\gamma)}{\lambda_0 b_l}\right)^{\frac{1}{l}}. \end{cases}$$

Finally, (16) is obtained using the joint p.d.f., $f_{R_1,R_2}(r_1, r_2) = (\lambda_0 b_l)^2 (r_1 r_2)^{l-1}\exp\left(-\frac{\lambda_0 b_l}{l}r_2^l\right)$, $0 \leq r_1 \leq r_2 \leq \infty$, due to the properties of Poisson point processes.

G. Proof for Theorem 5

Let us consider the probability of the event that the interference due to all the BSs beyond the signal BS at a given distance R_1 is below a certain value, say, δ, for the case $\varepsilon = 2$.

$$\begin{aligned}
&\mathbb{P}\left(\left\{\sum_{k=2}^{\infty} R_k^{-2} \leq \delta \,\middle|\, R_1\right\}\right) \\
&= \mathbb{P}\left(\left\{\mathrm{e}^{-s\sum_{k=2}^{\infty}R_k^{-2}} \geq \mathrm{e}^{-s\delta} \,\middle|\, R_1\right\}\right) \\
&\overset{(a)}{\leq} \mathrm{e}^{s\delta}\mathbb{E}\left[\mathrm{e}^{-s\sum_{k=2}^{\infty}R_k^{-2}} \,\middle|\, R_1\right] \\
&\overset{(b)}{=} \mathrm{e}^{s\delta}\mathrm{e}^{-\lambda\int_{r=R_1}^{\infty}\left(1-\mathrm{e}^{-sr^{-2}}\right)2\pi r dr} \\
&\overset{(c)}{=} \mathrm{e}^{s\delta}\mathrm{e}^{\lambda\int_{r=R_1}^{\infty}\sum_{k=1}^{\infty}\frac{\left(-sr^{-2}\right)^k}{k!}2\pi r dr} \\
&= \mathrm{e}^{s\delta}\mathrm{e}^{-\lambda s 2\pi\cdot\log(r)|_{r=R_1}^{\infty} + \lambda 2\pi\sum_{k=2}^{\infty}\frac{(-s)^k}{k!}\frac{\left(R_1^{2-k\varepsilon}\right)}{k\varepsilon - 2}} \\
&= \mathrm{e}^{s\delta}\times 0\times \mathrm{e}^{\alpha(R_1)} = 0,
\end{aligned}$$

where (a) is obtained by applying Markov's inequality; (b) is obtained by applying Campbell's theorem to the homogeneous Poisson point process defined in the 2-D plane beyond R_1 from the origin; (c) is obtained after the Taylor's series expansion of the exponential function in (b); and finally the result is obtained by noting that the exponential of a sum of functions is a product of exponential and by showing that one of the terms in the product is 0 while the others evaluate to a finite number.

As a result,

$$\mathbb{P}\left(\{SIR>\gamma\}\right) = \mathbb{E}_{R_1}\left[\mathbb{P}\left(\left\{\sum_{k=2}^{\infty} R_k^{-\varepsilon} < \left(\gamma R_1^{\varepsilon}\right)^{-1} \middle| R_1\right\}\right)\right]$$
$$= 0,\ \forall\, \gamma \geq 0.$$

and hence we have proved the result.

H. Simulation Methods

In this section, the details of simulating the SCS are presented. A single trial in simulating the BS placement for the 1-D SCS with BS density function $\lambda(r)$ in the region of interest which is a subset of the 1-D plane denoted by S, involves the following steps:

1) Generate a random number M, according to a Poisson distribution with mean $\int_S \lambda(s)ds$, which is the number of BSs to be placed in S for the given trial.
2) *BS placement*: For *homogeneous* 1-D SCS, generate M random numbers according to a uniform distribution in the range of S. If $\lambda(s)$ does not correspond to a *homogeneous* 1-D SCS, if $\lambda_{\max} = \sup_{s \in S} \lambda(s)$, then generate a random number y which is uniformly distributed in the range $[0, \lambda_{\max}]$ and another random number x according to a uniform distribution in the range of S. A BS is placed uniformly at x, only if $y < \lambda_0(x)$. This process is repeated until M BS are placed.
3) Compute the received power at the MS for each BS using the path-loss exponent ε. The fading in the SCS is incorporated by multiplying each of the received powers with i.i.d. random number generated according to the distribution of the fading factor. Finally, SINR at the MS corresponding to this trial, is computed according to (2).

For all the simulations in this paper $T = 100,000$ trials are used unless specified otherwise.

REFERENCES

[1] J. F. C. Kingman, *Poisson Processes (Oxford Studies in Probability)*. New York, NY, USA: Oxford Univ. Press, Jan. 1993.
[2] D. Stoyan, W. S. Kendall, and J. Mecke, *Stochastic Geometry and Its Applications*. Hoboken, NJ, USA: Wiley, 1995.
[3] D. J. Daley and D. Vere-Jones, *An Introduction to the Theory of Point Processes*, vol. 2, *General theory and structure*, 2nd ed. New York, NY, USA: Springer-Verlag, 2008, ser. Probability and Its Applications. [Online]. Available: http://www.springerlink.com/content/978-0-387-21337-8
[4] D. J. Daley and D. Vere-Jones, *An Introduction to the Theory of Point Processes*, vol. 1, *General theory and structure*, 2nd ed. New York, NY, USA: Springer-Verlag, 2008, ser. Probability and Its Applications. [Online]. Available: http://www.springerlink.com/content/978-0-387-21337-8
[5] T. X. Brown, "Cellular performance bounds via shotgun cellular systems," *IEEE J. Sel. Areas Commun.*, vol. 18, no. 11, pp. 2443–2455, Nov. 2000.
[6] T. X. Brown, "Analysis and coloring of a shotgun cellular system," in *Proc. IEEE RAWCON*, Aug. 1998, pp. 51–54.
[7] J. Andrews, F. Baccelli, and R. Ganti, "A tractable approach to coverage and rate in cellular networks," *IEEE Trans. Commun.*, vol. 59, no. 11, pp. 3122–3134, Nov. 2011.
[8] J. G. Andrews *et al.*, "Rethinking information theory for mobile ad hoc networks," *IEEE Commun. Mag.*, vol. 46, no. 12, pp. 94–101, Dec. 2008.
[9] S. Weber, X. Yang, J. G. Andrews, and G. de Veciana, "Transmission capacity of wireless ad hoc networks with outage constraints," *IEEE Trans. Inf. Theory*, vol. 51, no. 12, pp. 4091–4102, Dec. 2005.
[10] F. Baccelli and B. Błaszczyszyn, *Stochastic Geometry and Wireless Networks, Volume I—Theory*, vol. 3. Delft, The Netherlands: Now Publishers, 2009, ser. Foundations and Trends in Networking, no. 3/4.
[11] F. Baccelli and B. Błaszczyszyn, *Stochastic Geometry and Wireless Networks, Volume II—Applications*, vol. 4. Delft, The Netherlands: Now Publishers, 2009, ser. Foundations and Trends in Networking, no. 1/2.
[12] M. Haenggi and R. K. Ganti, *Interference in Large Wireless Networks*, vol. 3. Delft, The Netherlands: Now Publishers, 2008, no. 2
[13] M. Haenggi, J. Andrews, F. Baccelli, O. Dousse, and M. Franceschetti, "Stochastic geometry and random graphs for the analysis and design of wireless networks," *IEEE J. Sel. Areas Commun.*, vol. 27, no. 7, pp. 1029–1046, Sep. 2009.
[14] N. Jindal, J. G. Andrews, and S. Weber, "Bandwidth partitioning in decentralized wireless networks," *IEEE Trans. Wireless Commun.*, vol. 7, no. 12, pp. 5408–5419, Dec. 2008.
[15] M. Franceschetti, O. Dousse, D. Tse, and P. Thiran, "Closing the gap in the capacity of wireless networks via percolation theory," *IEEE Trans. Inf. Theory*, vol. 53, no. 3, pp. 1009–1018, Mar. 2007.
[16] P. Madhusudhanan, J. Restrepo, Y. Liu, and T. Brown, "Downlink coverage analysis in a heterogeneous cellular network," in *Proc. IEEE GLOBECOM*, Dec. 2012, pp. 4170–4175.
[17] P. Madhusudhanan, J. G. Restrepo, Y. E. Liu, T. X. Brown, and K. R. Baker, "Stochastic ordering based carrier-to-interference ratio analysis for the shotgun cellular systems," *IEEE Wireless Commun. Lett.*, vol. 1, no. 6, pp. 565–568, Dec. 2012.
[18] P. Madhusudhanan, J. G. Restrepo, Y. Liu, T. X. Brown, and K. Baker, "Multi-tier network performance analysis using a shotgun cellular system," in *Proc. IEEE GLOBECOM Wireless Commun. Symp.*, Dec. 2011, pp. 1–6.
[19] P. Madhusudhanan, J. G. Restrepo, Y. Liu, T. X. Brown, and K. Baker, "Modeling of interference from cooperative cognitive radios for low power primary users," in *Proc. IEEE GLOBECOM Wireless Commun. Symp.*, 2010, pp. 1–6.
[20] B. Błaszczyszyn, M. K. Karray, and H. P. Keeler, "Using Poisson processes to model lattice cellular networks," in *Proc. IEEE INFOCOM*, 2013, pp. 773–781.
[21] M. Haenggi, *Stochastic Geometry for Wireless Networks*. Cambridge, U.K.: Cambridge Univ. Press, 2013.
[22] S. Mukherjee, *Analytical Modeling of Heterogeneous Cellular Networks: Geometry, Coverage, Capacity*. Cambridge, U.K.: Cambridge Univ. Press, 2014.
[23] S. Weber and J. G. Andrews, "Transmission capacity of wireless networks," in *Foundations and Trends in Networking*, vol. 5. Delft, The Netherlands: Now Publishers, Jan. 2012.
[24] H. Takagi and L. Kleinrock, "Optimal transmission ranges for randomly distributed packet radio terminals," *IEEE Trans. Commun.*, vol. COM-32, no. 3, pp. 246–257, Mar. 1984.
[25] M. Zorzi and S. Pupolin, "Outage probability in multiple access packet radio networks in the presence of fading," *IEEE Trans. Veh. Technol.*, vol. 43, no. 3, pp. 604–610, Aug. 1994.
[26] S. M. Ross, *Stochastic Processes*. Hoboken, NJ, USA: Wiley, 1983.
[27] M. Shaked and J. G. Shanthikumar, *Stochastic Orders*. New York, NY, USA: Springer-Verlag, 2007, ser. Springer Series in Statistics.
[28] M. Shaked and J. G. Shanthikumar, *Stochastic Orders and Their Applications (Probability and Mathematical Statistics)*. San Diego, CA, USA: Academic, 1994.
[29] P. Madhusudhanan, J. G. Restrepo, Y. E. Liu, and T. X. Brown, "Carrier to interference ratio analysis for the shotgun cellular system," in *Proc. IEEE GLOBECOM Wireless Commun. Symp.*, Honolulu, HI, USA, Nov. 2009, pp. 1–6.
[30] H. P. Keeler, B. Błaszczyszyn, and M. K. Karray, "SINR-based k-coverage probability in cellular networks with arbitrary shadowing," in *Proc. IEEE ISIT*, 2013, pp. 1167–1171.
[31] A. M. Mathai and H. J. Haubold, *Special Functions for Applied Scientists*. New York, NY, USA: Springer-Verlag, Mar. 2008.
[32] H. S. Dhillon, R. K. Ganti, F. Baccelli, and J. G. Andrews, "Modeling and analysis of K-tier downlink heterogeneous cellular networks," *IEEE J. Sel. Areas Commun.*, vol. 30, no. 3, pp. 550–560, Apr. 2012.
[33] T. Q. S. Quek, G. de la Roche, I. Güvenç, and M. Kountouris, *Small Cell Networks—Deployment, PHY Techniques, Resource Management*. Cambridge, U.K.: Cambridge Univ. Press, 2013.
[34] R. Menon, R. Buehrer, and J. Reed, "On the impact of dynamic spectrum sharing techniques on legacy radio systems," *IEEE Trans. Wireless Commun.*, vol. 7, no. 11, pp. 4198–4207, Nov. 2008.
[35] C.-H. Lee and M. Haenggi, "Interference and outage in poisson cognitive networks," *IEEE Trans. Wireless Commun.*, vol. 11, no. 4, pp. 1392–1401, Apr. 2012.

[36] R. Dhillon and T. X. Brown, “Models for analyzing cognitive radio interference to wireless microphones in TV bands,” in *Proc. 3rd IEEE Symp. New Frontiers Dyn. Spectr. Access Netw.*, Oct. 2008, pp. 1–10.

[37] X. Hong, C.-X. Wang, and J. Thompson, “Interference modeling of cognitive radio networks,” in *Proc. IEEE Veh. Technol. Conf.*, May 2008, pp. 1851–1855.

[38] P. Madhusudhanan, T. Brown, and Y. Liu, “On the interference due to cooperative cognitive radios in the presence of multiple low-power primary users,” in *Proc. 49th Annu. Allerton Conf. Commun., Control, Comput.*, Sep. 2011, pp. 1657–1664.

[39] V. Chandrasekhar and J. Andrews, “Uplink capacity and interference avoidance for two-tier femtocell networks,” *IEEE Trans. Wireless Commun.*, vol. 8, no. 7, pp. 3498–3509, Jul. 2009.

[40] P. Xia, V. Chandrasekhar, and J. Andrews, “Open vs. closed access femtocells in the uplink,” *IEEE Trans. Wireless Commun.*, vol. 9, no. 12, pp. 3798–3809, Dec. 2010.

[41] P. Madhusudhanan, J. G. Restrepo, Y. Liu, and T. X. Brown, “Heterogeneous cellular network performance analysis under open and closed access,” in *Proc. IEEE GLOBECOM*, Dec. 2012, pp. 1–6.

[42] H. Dhillon, R. Ganti, and J. Andrews, “Load-aware modeling and analysis of heterogeneous cellular networks,” *IEEE Trans. Wireless Commun.*, vol. 12, no. 4, pp. 1666–1677, Apr. 2013.

[43] H.-S. Jo, Y. J. Sang, P. Xia, and J. Andrews, “Heterogeneous cellular networks with flexible cell association: A comprehensive downlink SINR analysis,” *IEEE Trans. Wireless Commun.*, vol. 11, no. 10, pp. 3484–3495, Oct. 2012.

[44] S. Mukherjee, “Distribution of downlink SINR in heterogeneous cellular networks,” *IEEE J. Sel. Areas Commun.*, vol. 30, no. 3, pp. 575–585, Apr. 2012.

[45] P. Pinto, A. Giorgetti, M. Win, and M. Chiani, “A stochastic geometry approach to coexistence in heterogeneous wireless networks,” *IEEE J. Sel. Areas Commun.*, vol. 27, no. 7, pp. 1268–1282, Sep. 2009.

[46] B. Błaszczyszyn and H. P. Keeler, “Equivalence and comparison of heterogeneous cellular networks,” in *Proc. PIMRC—WDN-CN*, 2013, pp. 153–157.

[47] H. S. Dhillon and J. G. Andrews, “Downlink rate distribution in heterogeneous cellular networks under generalized cell selection,” *IEEE Wireless Commun. Lett.*, vol. 3, no. 1, pp. 42–45, Feb. 2014.

Prasanna Madhusudhanan received the B.E. degree in telecommunication engineering from Visvesvaraya Technological University, Belgaum, India, in 2006 and the M.S. and Ph.D. degrees from the University of Colorado, Boulder, CO, USA, in 2010 and 2013, respectively. Since September 2013, he has been with Qualcomm Inc., Boulder. His research interests include communication theory, wireless networks, stochastic geometry, and dynamical systems.

Juan G. Restrepo received the B.S. degree in physics from the University of Los Andes, Bogotá, Colombia, in 1999 and the Ph.D. degree in applied mathematics from the University of Maryland, College Park, MD, USA, in 2005. He is currently an Assistant Professor with the Department of Applied Mathematics, University of Colorado, Boulder, CO, USA. His research interests include dynamical systems, chaos, synchronization of coupled oscillators, dynamics on complex networks, and cardiac dynamics.

Youjian (Eugene) Liu (S’98–M’01) received the B.E. degree in electrical engineering from Beijing University of Aeronautics and Astronautics, Beijing, China, in 1993; the M.S. degree in electronics from Beijing University, Beijing, in 1996; and the M.S. and Ph.D. degrees in electrical engineering from The Ohio State University, Columbus, OH, USA, in 1998 and 2001, respectively. From January 2001 to August 2002, he worked on space–time communications for 3G mobile communication systems as a Member of the Technical Staff in CDMA System Analysis and Algorithms Group, Wireless Advanced Technology Laboratory, Lucent Technologies, Bell Labs Innovations, Whippany, NJ, USA. Since August 2002, he has been with the Department of Electrical and Computer Engineering, University of Colorado, Boulder, CO, USA, where he is currently an Associate Professor. His current research interests include network communications, information theory, and coding theory.

Timothy X Brown received the B.S. degree in physics from Pennsylvania State University, State College, PA, USA, and the Ph.D. degree in electrical engineering from California Institute of Technology, Pasadena, CA, USA, in 1990. He is currently a Professor of electrical, computer, and energy engineering with the Interdisciplinary Telecommunications Program, University of Colorado, Boulder, CO, USA. Since 2013, he has been a Visiting Professor of electrical and computer engineering with Carnegie Mellon University in Rwanda, Kigali, Rwanda. His research funding comes from the NSF, FAA, DOE, and several industries. Projects include the role of mobility in network control of unmanned aircraft, denial of service vulnerabilities in wireless protocols, spectrum policy frameworks for cognitive radios, and indoor wireless network performance. His research interests include adaptive network control, machine learning, and wireless communication systems. He received the NSF CAREER Award and the GWEC Wireless Educator of the Year Award.

Kenneth R. Baker (SM’07) received the Ph.D. degree in electrical engineering from Virginia Polytechnic Institute and State University, Blacksburg, VA, USA, in 1993. He is currently a Scholar in Residence with the Interdisciplinary Telecommunications Program, College of Engineering and Applied Science, University of Colorado, Boulder, CO, USA. Prior to joining the University of Colorado, he held various wireless industry positions related to new product development and radio access network planning. He continues to contribute to the wireless industry through consultations, training, and system engineering. He is a holder of 13 patents in wireless communication system technology. His research interests include applications and methods related to self-configuring wireless networks, such as dynamic spectral reuse, multitier networks, propagation in random media, scheduling algorithms for the wireless channel, and cross-layer adaptive antenna techniques. This work incorporates software-defined radio technology for network performance validation. His teaching interests include communications theory, networking concepts and protocols, and digital wireless communication signal processing.